

# An Energy Efficient Resource Allocation Scheme Based on Cloud-Computing in H-CRAN

Ximu Zhang, Min Jia, *Senior Member, IEEE*, Xuemai Gu, *Member, IEEE*, Qing Guo, *Member, IEEE*.

**Abstract**—Compared with the cloud radio access network (C-RAN), heterogeneous cloud radio access network (H-CRAN) with the high-power node (HPN) entity which separates the control and broadcast functionalities from the baseband processing unit (BBU) pool. It makes the user access, resource allocation, load balancing more flexible, which also makes the intra-layer interference and inter-layer interference more complex. Therefore, the heavy inverse operations for dense matrixes and the complicated power allocation algorithms in beamforming perform large floating-point calculations per second (FLOPS) in BBU pool. As frequency resources grow scarcer, green communication with high energy efficiency and low carbon emissions has raised significant concerns. In this paper, we focus on the energy efficiency (EE) advantages achieved by selectively cooperative transmission and associated power consumption model. A joint channel matrix sparseness and normalized water-filling resource allocation algorithm is proposed and formulated to improve energy efficiency at different user density through mathematical derivation. By reducing the computation complexity of cooperative transmission, the proposed scheme decreases the digital baseband power consumption, which is more adaptable for tidal phenomenon. Simulation results show that the proposed algorithm can effectively reduce the energy consumption of baseband and improve the energy efficiency of the system.

**Index Terms**—IoT, heterogeneous cloud radio access network, energy efficiency, cooperative transmission, channel matrix sparseness, green communications.

## I. INTRODUCTION<sup>1</sup>

With explosive growth of the Internet of Things (IoT) business, cloud computing provides an effective solution for the massive data calculation and storage[1]-[3]. IoT can be considered as a platform for cloud computing technology. As cloud computing has made significant progress, IoT can better

enhance data storage and processing capabilities [4]. Without the powerful support from cloud computing, IoT performance will undoubtedly be greatly reduced. Therefore, the IoT has a strong dependence on cloud computing.

As frequency resources grow scarcer, green communication with high energy efficiency and low carbon emissions has become one of the research hotspots [5], [6]. With the popularity of ultra-high-definition video streaming, augmented reality (AR), virtual reality (VR) and other technologies, 5G networks will face large data traffic, scarce spectrum resources and high energy consumption challenges [7]-[10]. Due to the rapid development of the telecom industry, massive user access has become the focus of attention [11], [12]. The energy-efficient wireless communication will bring sustainable benefits, therefore, the United States explicitly proposed to reduce the energy consumption by 25% before 2030 and the United Kingdom set an objective for reducing energy consumption by 50% before 2050. H-CRAN as a green wireless access network architecture based on centralized processing, collaborative radio and real-time cloud infrastructure which can improve the energy efficiency and achieve flexible access, where the users are accessed to baseband unit (BBU) pool via the fiber optics and cooperated in BBU pool [13], [14].

Access technology is the core of the Internet of things, which include Ethernet technology, WLAN technology, Bluetooth technology, Zigbee technology[15]. H-CRAN will be the most important access method in the field of IoT. The HPN entity is embedded in H-CRAN system, which can control information distribution in the whole network and separate the centralized control cloud function from BBU pool [16], [17]. The BBU pool is connected to the macro base station via the S1 and X2 interfaces. H-CRAN can use the cell-range shrink technology in HETNET to balance the users between remote radio head (RRH) and HPN, where HPN provides seamlessly cover burst communications business or instant messaging services and RRHs support local service through the RRHs adaptive access to BBU processing pool. From the access mode aspect, 5G will achieve satellite access and a smooth transition from C-RAN to H-CRAN [18], [19]. Some RRHs enter the sleep mode through the centralized self-optimization in BBU pool when the number of active users decreases. When the traffic loads are high, active users can adaptively activate the sleep mode RRH. Therefore, one or more RRHs are adaptable access to BBU pool according to requirements of transmission performance [20]. Although one

Manuscript is received 16, September, 2018. This work was supported by the National Natural Science Foundation of China under Grant 61671183, Grant 61771163, and the Open Research Fund of CETC key laboratory of aerospace information applications under Grant SXX18629T022. (Corresponding author: Min Jia.)

Ximu Zhang, Min Jia, Xuemai Gu, Qing Guo are with the Communication Research Center, School of Electronics and Information Engineering, Harbin Institute of Technology, Harbin, 150080, China (e-mail: zhangximu@stu.hit.edu.cn; jiamin@hit.edu.cn; guxuemai@hit.edu.cn; qguo@hit.edu.cn). Ximu Zhang is also with CETC key laboratory of aerospace information applications.

Copyright (c) 2012 IEEE. Personal use of this material is permitted. However, permission to use this material for any other purposes must be obtained from the IEEE by sending a request to pubs-permissions@ieee.org.

of the top EE power allocation scheme has been proposed in [21], the extra complexity of matrix inverse operations is neglected in the process of beamforming. FLOPS in the process of power allocation is calculated in [22], [23]. However, the baseband processing power consumption is not considered in whole power consumption model and the energy efficiency is not accurate.

A green resource allocation scheme for the downlink of H-CRANs between RRHs has been proposed in [24], and their associated UEs aims at maximizing energy efficiency while satisfying the UE QoS requirements and mitigating the inter-tier interference. In addition, the energy-efficient optimization problem with delay constraint of C-RAN is proposed in [25]. To deal with the optimization problem, a non-linear fractional programming was formulated. However, the power consumption model is not comprehensive.

Due to the increased interference caused by intensive deployment of RRH, the beamforming algorithm is used in [26], [27] to reduce the interference among RRHs. However, the proposed beamforming algorithm in [28] reduces the inter-cell interference, the throughput, effective coverage area and energy efficiency of the resource allocation scheme in HETNET are not ideal. The work in [29], [30] employs an optimal power allocation scheme with great throughput improvement, but energy efficiency is still poor.

In this paper, an energy-efficient resource allocation scheme in the framework of H-CRAN model is proposed. First, the power consumption model is established. Based on this model, selective beamforming with channel matrix sparseness algorithm is then proposed to improve the energy efficiency in coordinated multi-point (CoMP) transmissions without regarding to small interference to noise ratio (INR) between some micro base stations and users. Finally, the numerical results show that the proposed energy efficiency scheme is superior to the traditional scheme. H-CRAN can efficiently decrease energy consumption.

The main contributions are summarized as follows:

- Matrix sparseness (MS) is proposed to reduce the computational complexity, which leads to lower digital baseband power consumption  $P_{BB}$  and higher EE in H-CRAN. Furthermore, a resource allocation algorithm combining MS and normalized Water-Filling (MSNWF) are proposed for providing efficiency and has robust performance in terms of throughput and EE.
- We apply proposed resource allocation scheme in H-CRAN, and thus users are accessed to BBU pool via the fiber optics and cooperated intra-layer in BBU pool. Then, we proposed power consumption model that applies to H-CRAN. Simulation results illustrate that H-CRAN can achieve flexible access and improve the energy efficiency and throughput in comparison to C-RAN.
- The algorithm complexity analysis is conducted for MSNWF and OPT. It performs a significant reduction comparing to OPT. Thus MSNWF algorithm has advantages in such sectors as complexity, power consumption and EE.

The rest of the paper is organized as follows. Section II introduces the H-CRAN system model and power consumption

model. The detail of problem formulation is also introduced. Section III describes the proposed MSNWF and its complexity is analyzed. In Section VI, the simulation results are presented and discussed. Finally, Section V concludes this paper.

## II. SYSTEM MODEL AND PROBLEM FORMULATION

### A. Architecture of H-CRAN based on "tidal phenomenon"

H-CRAN architecture offers huge potential to mitigate interference through cooperative transmission. The optical medium through radio signal between RRHs and the BBU will be carried, which can bring additional benefits in supporting centralized signal processing through data exchange in BBU pool. H-CRAN is composed of four elements such as HPN, remote radio head (RRH), baseband unit (BBU) and optical fibers.

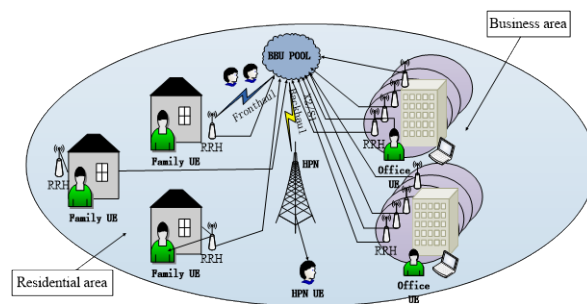


Fig.1 H-CRAN architecture in a macro/femto HETNET

The H-CRAN architecture shown in Fig.1 takes full advantage of both C-RANs and HETNET, which offers tremendous potential to facilitate collaborative transmission to mitigate interlayer interference.

1) RRHs: Distributed radio units located at remote sites, with cloud processing and computing capabilities moved to the BBU.

2) BBU: A cloud-based platform where signals are processed by real-time virtualized computing resources. Therefore, H-CRAN is more conducive to cooperative transmission in the BBU processing pool.

3) HPN: HPN acts as traditional macro BS, which controls information distribution in the whole network and separates the control and broadcast functionalities from the baseband processing unit (BBU) pool.

4) Optical fibers: The optical medium through which radio signal between RRH and BBU will be carried. This medium allows low-power signals to travel farther faster and be deployed as in practice a passive optical network (PON) for cost-effectiveness [28].

Therefore, H-CRAN has the following advantages.

1) Fronthaul capacity: The BBU pool is connected to the macro base station via the S1 and X2 interfaces. Therefore, H-CRAN controls information distribution in the whole network and separates the centralized control cloud function from the baseband processing unit (BBU) pool effectively and efficiently.

2) Cognition and dynamic cooperation: H-CRAN can use the cell-range shrink technology in HETNET to balance the load

between RRH and HPN.

3) Green communication: When the number of active users is small, some RRHs enter the sleep mode under the centralized self-optimization of the BBU pool. When the traffic loads are high, active users can adaptively activate the sleep mode RRH. H-CRAN can decrease energy consumption which is more in line with green communication objective [32].

The H-CRAN architecture can not only adapt to the small-scale migrate from the factory to the dormitory back and forth, but also can correspond to the large-scale office workers from the suburban housing to the city center office back and forth. This effect is also known as the "tidal phenomenon", which is characterized by the total number of active users in the network unchanged in different periods of time in the office area (work) or residential area (get off work).

### B. Power Consumption Model

The power amplifier in the H-CRAN is only considered in the power consumption model proposed in [33] while the power consumption of the baseband processing, system overhead, radio frequency, etc. are ignored. The proposed power consumption model in [34] includes power consumption generated by amplifier, baseband processing, system overhead, radio frequency, but it can not be applied to H-CRAN. In this paper, a power consumption model for H-CRAN scenarios is proposed, which is composed of six modules such as power amplifier, baseband processing, system overhead, radio frequency, backhaul and fronthaul.

Based on the European EARTH project [35], an energy consumption model for C-RAN networks is proposed, which is divided into four modules such as digital baseband  $P_{BB}$ , power amplifier  $P_{PA}$ , radio frequency  $P_{RF}$  and system overhead  $P_{OV}$ .

$$P_{BB} = P_S(1 + \eta_{Leak}) \quad (1)$$

where  $P_S$  is the baseband-processor power,  $\eta_{Leak}$  is the compensation for COMS leakage current.

$$P_{PA} = N_{TX} \frac{P_{TX}}{\eta_{PA}(1 - \sigma_{feed})} \quad (2)$$

where  $N_{TX}$  is the active antenna number,  $P_{TX}$  is the antenna transmitting power,  $\eta_{PA}$  is the efficiency of the power amplifier and  $\sigma_{feed}$  is the loss of feeder link.

$$P_{OV} = (P_{BB} + P_{RF} + P_{PA}) \cdot ((1 + \eta_{cool})(1 + \eta_{dc}) - 1) \quad (3)$$

where  $\eta_{cool}$  is the cooling coefficient,  $\eta_{dc}$  is the power coefficient and  $\eta_{acdc}$  is the current conversion coefficient.

The specific subcomponents and the reference values in each module and the adjustment criteria in the actual communication process are given in [35], in order to calculate the actual energy consumption of C-RAN.

$$P_{tot}^c = P_{BB} + P_{RF} + P_{PA} + P_{OV} \quad (4)$$

$P_{tot}^c$  is the actual energy consumption of C-RAN. Moreover, RRH fronthaul and backhaul power consumption are represented by  $PC_n^r(t)$  and  $PF_n^r(t)$  in H-CRAN, respectively.

RRH backhaul power consumption is represented by  $PF_n^r(t)$ . The optical/electrical common public radio interface (CPRI) is used for fronthaul and backhaul links on both sides of the RRH and BBU. According to the chip manual [35], each CPRI interface consumes 1.5 watts.

HPN fronthaul power consumption is represented by  $PC_n^M(t)$ . HPN backhaul power consumption is represented by  $P_n^M F_n(t)$ . The optical/electrical interface X2/S1 is used for fronthaul and backhaul links on both sides of the HPN and BBU. Therefore, the total network power consumption in H-CRAN can be expressed as:

$$P_{tot}^h = P_{BB} + P_{RF} + P_{PA} + P_{OV} + PC_n^M(t) + P_n^M F_n(t) \quad (5)$$

where  $PC_n^M(t)$  and  $P_n^M F_n(t)$  are the circuit power consumption and fronthaul consumption, respectively. The work in [16] argues that the backhaul/ fronthaul power of HPN is too small to care. Because the optical fibers allow low-power signals to travel farther faster. In addition, the size of  $PC_n^R(t)$ ,  $PC_n^M(t)$ ,  $P_{RF}$  and  $P_{OV}$  are determined in the chip manual and other hardware parameters are fixed[34]. Therefore, the network energy consumption in H-CRAN can be reduced as:

$$P_{tot}^h = P_S(1 + \eta_{Leak}) + N_{TX} \frac{P_{TX}}{\eta_{PA}(1 - \sigma_{feed})} \quad (6)$$

### C. Problem Formulation

The downlink H-CRAN system shown in Fig 1 includes an HPN and  $N$  RRHs. Centralized control cloud is in HPN and centralized logic storage cloud and centralized logic communication cloud are in BBU pool. In the downlink process, RRHs have serious intra-layer interference in the BBU pool. The BBU pool generates a large amount of baseband energy consumption. An HPN and  $n$  RRHs can be sorted by  $N = \{0, 1, \dots, n\}$ . Define the set of RUEs as  $K_R = \{1, 2, \dots, K_R\}$ , and the set of HUEs as  $K_H = \{1, 2, \dots, K_H\}$ .  $\mathbf{h}_k(t)$  denotes the Channel State Information (CSI) matrix from all RRHs' transmit antennas to user equipment  $k$  and  $\mathbf{g}_{0,k}(t)$  denotes the CSI matrix from the HPN's transmit antennas to user equipment  $k$ . The received signal at the RRH user equipment (RUE)  $k$ , can be expressed as

$$Y_k(t) = \mathbf{h}_k^H(t) \mathbf{w}_k(t) S_k(t) + \sum_{j=1, j \neq k}^{K_R} \mathbf{h}_k^H(t) \mathbf{w}_j(t) S_j(t) + \sum_{i=1}^{K_H} \mathbf{g}_{0,k}^H(t) \mathbf{w}_{0,i}(t) S_i(t) + n_{if} \quad (7)$$

where RRH downlink channel matrix for the  $k$  th user is represented by  $\mathbf{h}_k(t)$  and HPN downlink channel matrix for the  $k$  th user is represented by  $\mathbf{g}_{0,k}(t)$ . HPN, Office RRH and

family RRH downlink beamforming vector for the  $k$ th user are represented by  $\mathbf{w}_k(t)$ . In particular, the transmit beamformer from the HPN to user equipment  $k$  is denoted by  $\mathbf{w}_{0,k}(t)$ .  $n_{if}$  is the receiver noise at RUE  $k$ . It is assumed that the scalar-valued data stream  $S_k(t)$  is temporally white with zero mean and unit variance.

As a result, according to the Shannon capacity formula, the achieved transmission rate for RUE  $k$  can be expressed as

$$C_k(t) = B \log_2 \left( 1 + \frac{\mathbf{w}_k^H(t) \mathbf{h}_k(t) \mathbf{h}_k^H(t) \mathbf{w}_k(t)}{\sum_{j=1, j \neq k}^{K_R} \mathbf{h}_k^H(t) \mathbf{w}_j(t) \mathbf{w}_j^H(t) \mathbf{h}_k(t) + \sum_{i=1}^{K_H} \mathbf{g}_{0,k}^H(t) \mathbf{w}_{0,i}(t) \mathbf{w}_{0,i}^H(t) \mathbf{g}_{0,k}(t) + \sigma^2} \right) \quad (8)$$

The received signal at the HPN user equipment (HUE)  $k$ , can be expressed as

$$Y_k(t) = \mathbf{g}_{0,k}^H(t) \mathbf{w}_{0,k}(t) S_k(t) + \sum_{i=1, i \neq k}^{K_H} \mathbf{g}_{0,k}^H(t) \mathbf{w}_{0,i}(t) S_i(t) + \sum_{j=1}^{K_R} \mathbf{h}_k^H(t) \mathbf{w}_j(t) S_j(t) + n_{if} \quad (9)$$

where RRH downlink channel matrix for the  $k$ th user is represented by  $\mathbf{h}_k(t)$  and HPN downlink channel matrix for the  $k$ th user is represented by  $\mathbf{g}_{0,k}(t)$ . As a result, according to the Shannon capacity formula, the achievable transmission rate for HPN  $k$  can be expressed as

$$C_k(t) = B \log_2 \left( 1 + \frac{\mathbf{g}_{0,k}^H(t) \mathbf{w}_{0,k}(t) \mathbf{w}_{0,k}^H(t) \mathbf{g}_{0,k}(t)}{\sum_{j=1, j \neq k}^{K_H} \mathbf{g}_{0,k}^H(t) \mathbf{w}_{0,j}(t) \mathbf{w}_{0,j}^H(t) \mathbf{g}_{0,k}(t) + \sum_{i=1}^{K_R} \mathbf{h}_k^H(t) \mathbf{w}_i(t) \mathbf{w}_i^H(t) \mathbf{h}_k(t) + \sigma^2} \right) \quad (10)$$

$P_{\text{tot}}^h$  is the network energy consumption. Based on H-CRAN power consumption model, the total power consumption of the system can be expressed as

$$P_{\text{tot}}^h = P_S(1 + \eta_{\text{Leak}}) + N_{\text{TX}} \frac{P_{\text{TX}}}{\eta_{\text{PA}}(1 - \sigma_{\text{feed}})} \quad (11)$$

If the inter-layer interference and the intralayer interference are coordinated by CoMP, zero-forcing precoding can be expressed as

$$\mathbf{h}_k^H(t) \mathbf{w}_i(t) = 0, \forall i \neq k \quad (12)$$

$$\mathbf{g}_{0,k}^H(t) \mathbf{w}_{0,l}(t) = 0, \forall l \neq k \quad (13)$$

The total throughput of H-CRAN system can be expressed as

$$C_k(t) = \sum_{k=1}^{K_R} B \log_2 \left( 1 + \frac{\mathbf{w}_k^H(t) \mathbf{h}_k(t) \mathbf{h}_k^H(t) \mathbf{w}_k(t)}{\sigma^2} \right) + \sum_{i=1}^{K_H} B \log_2 \left( 1 + \frac{\mathbf{w}_{0,i}^H(t) \mathbf{g}_{0,i}(t) \mathbf{g}_{0,i}^H(t) \mathbf{w}_{0,i}(t)}{\sigma^2} \right) \quad (14)$$

Total energy efficiency of the H-CRAN system can be expressed as

$$\eta_{\text{EE}} = \frac{C}{P_{\text{tot}}^h} = \frac{\sum_{k=1}^{K_R} B \log_2 \left( 1 + \frac{\mathbf{w}_k^H(t) \mathbf{h}_k(t) \mathbf{h}_k^H(t) \mathbf{w}_k(t)}{\sigma^2} \right) + \sum_{i=1}^{K_H} B \log_2 \left( 1 + \frac{\mathbf{w}_{0,i}^H(t) \mathbf{g}_{0,i}(t) \mathbf{g}_{0,i}^H(t) \mathbf{w}_{0,i}(t)}{\sigma^2} \right)}{P_S(1 + \eta_{\text{Leak}}) + N_{\text{TX}} \frac{P_{\text{TX}}}{\eta_{\text{PA}}(1 - \sigma_{\text{feed}})}} \quad (15)$$

The objective function and constraints are shown in equation (16).

$$\begin{aligned} & \max \eta_{\text{EE}} \\ & \text{s.t. } p_{\text{TX}}^i \leq p_{\text{TX max}}, \forall i \\ & p_{\text{TX}}^i \geq 0, \forall i \end{aligned} \quad (16)$$

where  $p_{\text{TX}}^i$  is the antenna transmitting power.  $p_{\text{TX max}}$  denotes the maximal antenna transmitting power. The objective function is to solve the problem that how to maximize the energy efficiency of cell under the premise of satisfying the service transmission characteristics.

### III. JOINT RESOURCE ALLOCATION ALGORITHM

#### A. Matrix Sparseness (MS)

The baseband processing power increases will directly affect the overall power consumption of the system and decrease the energy efficiency of the system. Due to the large scale fading in the urban environment, the interference to noise ratio (INR) between some RRHs and RUEs is too small to be considered. In the process of CoMP, a small number of adjacent offices RRHs/residential RRHs and RUEs have serious interference. In order to improve the energy efficiency in the CoMP process, a selective beamforming based on the channel matrix sparseness algorithm is proposed in this section.

According to the proposed power consumption model, the optimal objective function is deduced in H-CRAN. Then we propose a simple but efficient CoMP scheme to reduce the cooperation associated computation complexity. In the process of beamforming, the complexity of the algorithm is very high as the baseband processing pool needs to carry out matrix inverse operation.

According to (1), the baseband processing pool will generate a lot of power consumption. Then the energy efficiency of the H-CRAN system is reduced according to (15). The number of nonzero elements in the channel matrix is  $(R + ON_f + H)^2$ .

$R$  denotes the number of residential cell, and  $O$  denotes the number of office cell.  $N_f$  is the floor number of office building, and  $H$  is the number of HUE. When  $R$ ,  $H$  and  $O$  become larger, the inverse involve a large number of operations during the CoMP, leading to generate additional energy consumption in the baseband processing pool. Therefore, the matrix sparseness algorithm is proposed, which transforms the original channel matrix from the macroscopic base station and the micro-base station geographic distribution feature to the sparse matrix, which reduces the complexity of the matrix inversion operation.

Define the interference threshold the user can tolerate:  $\text{INR} > \beta$  (e.g.  $\beta = -30\text{dB}$  etc.). Collaboration users are picked out when INR is greater than threshold and the corresponding channel transition probability remains unchanged.

Set the channel matrix transition probability with  $\text{INR} \leq \beta$  to zero. Thus, the channel matrix  $H(t)$  changes from dense matrix to sparse matrix.

The channel gains of HPN and RRH are represented by  $h_n^{HPN}$  and  $h_n^{RRH}$  with antenna gain  $H_o^{HPN}$  and  $H_o^{RRH}$ . Channel gain for the  $n$ th user can be calculated as

$$h_n^{HPN} = \tilde{h}_n^{HPN} \xi H_o^{HPN} \left( \frac{d_o}{d_{HPN}} \right)^\alpha \quad (17)$$

$$h_n^{RRH} = \tilde{h}_n^{RRH} \xi H_o^{RRH} \left( \frac{d_o}{d_{RRH}(\phi)} \right)^\alpha \quad (18)$$

where  $d_o$  is reference distance,  $\tilde{h}_n^{HPN}$  and  $\tilde{h}_n^{RRH}$  are the rayleigh random variables,  $\alpha$  is the path loss constant and  $\xi$  is log normal shadowing.  $d_{HPN}$  and  $d_{RRH}(\phi)$  are the distances of user from HPN and RRH. The user that the RRH can not reach is communicating with the HPN. The user association is done based on best possible channel available.

The user association binary selection can be expressed as

$$\bar{h}_n = \lambda * h_n \quad (19)$$

$$\lambda_{i \neq j} = \begin{cases} 1, & INR > \beta \\ 0, & INR \leq \beta \end{cases} \quad (20)$$

where  $h_n$  is the channel gain for the  $n$ th user, and  $\bar{h}_n$  is adjusted channel gain for the  $n$ th user. As a binary indicator,  $\lambda$  is the estimated coefficient of the sub-channel.

It is necessary to inverse the channel matrix to find the pre-coding matrix in the beamforming process. The inverse matrix of  $\mathbf{H}(t)$  is  $\mathbf{G}(t)$ .

$\mathbf{H}(S_i)$  represents the downlink channel matrix between the user  $S_i$  and HPN/RRH. Perform the channel matrix  $\mathbf{H}(S_i)$  inversion to obtain the beamforming matrix  $\mathbf{G}(S_i)$ . The relationships of  $\mathbf{H}(S_i)$  and  $\mathbf{G}(S_i)$  follow the formula (21), which means  $\mathbf{G}(S_i)$  and  $\mathbf{H}(S_i)$  are pseudo inverse matrices

$$\mathbf{G}(S_i) \mathbf{H}(S_i) = \mathbf{I}_{|S_i|} \quad (21)$$

Basd on the beamforming matrix, actual transmission signal can be expressed as

$$x_i = \mathbf{G}(S_i) u_i \quad (22)$$

### B. Normalization Water-Filling (NWF)

It is observed in traditional HETNET that throughput and energy efficiency are low[36]. Literature [26] proposed a power allocation strategy(OPT) to meet the single antenna maximum transmit power of solving the following convex optimization problem under the premise. The algorithm achieves the system throughput optimization.

$$\begin{aligned} \max \quad & C = \sum_{f=0}^F \sum_{i=1}^{|S_i|} \log(1 + \frac{s_i}{\sigma^2}) \\ \text{s.t.} \quad & s_i \geq 0, i = 1, \dots, |S_i| \\ & \sum_{i=1}^{|S_i|} |g_{if}|^2 s_i \leq p_f^{\max}, i = 1, \dots, |S_i|, \forall f. \end{aligned} \quad (23)$$

However, the convex optimization algorithm described in (23) performs large complex operations at the base station processing side. In this section, a Normalization Water-Filling (NWF) power allocation strategy applied to H-CRAN is proposed, which is expected to reduce the complexity.

Normalize the transmission power and define the normalization factor

$$c = \sqrt{p_H^{\max} / p_R^{\max}} \quad (24)$$

where  $p_H^{\max}$  and  $p_R^{\max}$  are the maximum transmission power of the HPN and RRH respectively.

The channel gain between the HPN and the active user is multiplied by  $\sqrt{c}$ .

$$\tilde{\mathbf{H}}(:, 1) = c \cdot \hat{\mathbf{H}}(:, 1) \quad (25)$$

The transmission power of HPN is replaced by the transmission power of the microcellular base station RRHs.

And then, the distribution of each antenna power  $p_f, f = 0, 1, \dots, F$  is calculated according to the principle of water filling. Water filling algorithm through allocate the transmission power adaptively according to the channel condition [37]. We calculate the HPN transmit power  $P_{HPN}$ , office RRH transmit power  $P_{officeRRH}$ , home RRH transmit power  $P_{homeRRH}$  and power adjustment factor  $\lambda$  according to the channel condition  $H$ , normalization factor  $c$  and noise power  $N_0$ . Consequently, the final transmission power of the HPN is  $c\lambda p_f$  and the final transmission power of the RRHs are  $\lambda p_f$ .

Therefore, the resource allocation algorithm of MSNWF is described as follows.

---

#### Algorithm 1: MSNWF Resource Allocation Algorithm

---

##### Part 1: beamforming

- 1: Initialize  $H, \beta, \lambda$
- 2: if  $i = j$  then
- 3:  $\lambda_{ij} \leftarrow 1$
- 4: else
- 5:  $\lambda_{ij} = \begin{cases} 1, & INR > \beta \\ 0, & INR \leq \beta \end{cases}$
- 6:  $\bar{h}_n = \lambda \circ h_n$
- 7:  $\mathbf{G}(S_i) \bar{\mathbf{H}}(S_i) = \mathbf{I}_{|S_i|}$
- 8:  $x_i = \mathbf{G}(S_i) u_i$

##### Part 2: power allocation

- 1:  $c = \sqrt{p_H^{\max} / p_R^{\max}}$
  - 2:  $H(:, 1) \leftarrow H(:, 1) * c$
-

$$\begin{aligned}
 & \text{3: } (P_{\text{officeRRH}} \ P_{\text{homeRRH}} \ P_{\text{HPN}} \ \lambda) \xleftarrow{\text{WF}} \begin{cases} H \\ c \\ N_0 \end{cases} \\
 & \text{4: } P_{\text{HPN}} \leftarrow P_{\text{HPN}} * \lambda * c \\
 & \text{5: } P_{\text{officeRRH}} \leftarrow P_{\text{officeRRH}} * \lambda \\
 & \text{6: } P_{\text{homeRRH}} \leftarrow P_{\text{homeRRH}} * \lambda
 \end{aligned}$$

### C. Complexity analysis

This section analyzes and compares the complexity. The complexity of the proposed MSNWF is analyzed and compared with that for solving the convex optimization problem. For MS, the channel matrix denoted as  $\mathbf{H}(S_i)$ , which has  $(R + ON_f + H)^2$  non-zero elements, much more than  $\overline{\mathbf{H}}(S_i)$ .  $R$  denotes the number of residential cell, and  $O$  denotes the number of office cell.  $N_f$  is the floor number of office building, and  $H$  is the number of HUE.

For NWF, the water-filling process is much less complicated than solving the convex optimization problem as in (23). The flop count of beamforming process is determined by the extent of channel matrix sparseness, as summarized in Algorithm 1.

Assume that a sparse  $n \times n$  matrix  $\mathbf{H}$  can be expressed as

$$\mathbf{H} = \begin{bmatrix} \mathbf{a} & \mathbf{b}^T \\ \mathbf{c} & \mathbf{D} \end{bmatrix} \quad (26)$$

Schur complement  $S$  can be expressed as

$$s = \mathbf{a} - \mathbf{b}^T \mathbf{D}^{-1} \mathbf{c} \quad (27)$$

3n-2 flops are added to calculate Schur complement in formula 25. Inverse Schur complement  $s^{-1}$  added one flop. Therefore, beamforming matrix  $\mathbf{W}$  can be expressed as

$$\begin{aligned}
 \mathbf{W} = \mathbf{H}^{-1} &= \begin{bmatrix} s^{-1} & -s^{-1} \mathbf{b}^T \mathbf{D}^{-1} \\ -\mathbf{D}^{-1} \mathbf{c} s^{-1} & \mathbf{D}^{-1} + \mathbf{D}^{-1} \mathbf{c} s^{-1} \mathbf{b}^T \mathbf{D}^{-1} \end{bmatrix} \\
 &= \begin{bmatrix} s^{-1} & -s^{-1} \mathbf{b}^T \mathbf{D}^{-1} \\ -\mathbf{D}^{-1} \mathbf{c} s^{-1} & \mathbf{D}^{-1} + (-\mathbf{D}^{-1} \mathbf{c} s^{-1})(-s^{-1} \mathbf{b}^T \mathbf{D}^{-1}) s \end{bmatrix}
 \end{aligned} \quad (28)$$

In this process,  $n^2 + 3n + 1$  flops are added in problem (28). Therefore, the total floating-point operation count of MS equals to  $n^2 + 6n$  flops.

In part 2 of algorithm 1, one flop is added for defining the normalization factor in step 1.  $N$  flops are added for normalization channel matrix in power allocation and  $2n^2 + n \log_2 n + 5n$  flops are added in water-filling algorithm.  $N$  flops are added in step 5 and step 6, respectively.

Therefore, total flop of MSNWF  $3n^2 + n \log_2 n + 15n$  is far less than the total flop of OPT  $9n^3 + 6n^2 + n$ . Therefore, the computational complexity of the proposed method MSNWF has superiority in computational complexity against throughput convex optimization, and it can decrease the power consumption.

## IV. SIMULATION RESULTS

This section provides simulation results to prove that the proposed scheme outperforms others. According to the "tidal phenomenon", RRHs are divided into office RRH and residential RRH. The main components in H-CRAN consist of three modules: centralized BBU pool for baseband processing, HPN and RRHs represented by low power pico BSs. C-RAN including RRHs are connected to the BBU pool through optical fiber. HPN-tier, home RRH-tier and office RRH-tier are composed of HUE, home RUE and office RUE, respectively. The proposed algorithm is compared with two other schemes. In the centralized resource allocation approach, only one dell server is utilized as the controller and the unit for baseband processing [24]. OPT is proposed to maximize throughput through solving convex optimization problem with constraints related to transmit power. Compared with HETNET and OPT algorithms, throughput and energy efficiency of one-tier HPN, one-tier office RRH, one-tier house RRH, one-tier C-RAN and two-tier H-CRAN in different user activity are calculated respectively. Table I shows network parameters for simulation.

Table I  
H-CRAN SIMULATION PARAMETERS

Symbol	Implication	Value
$R$	The number of residential cell	40
$O$	The number of office building	15
$N_f$	The floor number of office building	4
$P_H^{\max}$	The maximum transmission power of HPN	46dBm
$P_R^{\max}$	The maximum transmission power of RRH	20dBm
$d_{\text{HPN}}^{\max}$	HPN maximum coverage	1km
$d_{\text{RRH}}^{\max}$	RRH maximum coverage	30m
$P_{\text{in}}$	The penetration losses of the signal strength due to inner walls	5dB
$P_{\text{out}}$	The penetration losses of the signal strength due to outer walls	10dB

### A. Throughput

To evaluate the throughput of the proposed scheme, we analyze the traditional C-RAN, HPN tier, one-office RRH tier, one-home RRH tier and two-tiers H-CRAN scenarios. Only one HPN is considered in the H-CRAN. In H-CRAN, RRHs are classified into office RRH and residential RRH.

HPN tier includes macro base stations and all macro base station users. In the One-tier C-RAN, the RRH users and HPN users cooperate at intra-layer. In the Two-tier H-CRAN, RUEs self-adaptive access to RRH and HUEs are connected with HPN. The RRHs users cooperate with HPN users inter-layer in H-CRAN.

In Office Hour, throughput performance comparisons among one-tier HPN, one-tier office RRH, one-tier house RRH, one-tier C-RAN, and two-tier H-CRAN are shown in Fig. 2 in three different schemes.



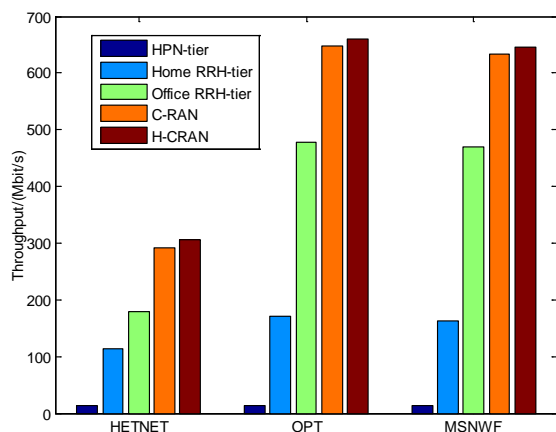


Fig.2 Throughput performance comparisons among one-tier HPN, one-tier office RRH, one-tier house RRH, one-tier C-RAN, and two-tier H-CRAN in "Office Hour".

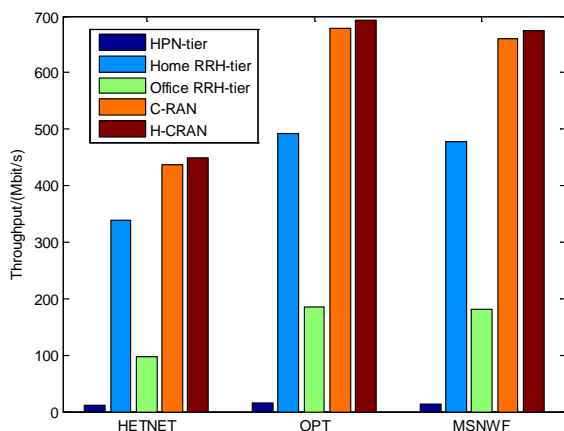


Fig.3 Throughput performance comparisons among one-tier HPN, one-tier office RRH, one-tier house RRH, one-tier C-RAN, and two-tier H-CRAN in "Family Hour".

In Family Hour, throughput performance comparisons among one-tier HPN, one-tier office RRH, one-tier house RRH, one-tier C-RAN and two-tier H-CRAN are shown in Fig. 3 in three different schemes.

The simulation results show that H-CRAN scene has higher throughput than traditional C-RAN scene. When the spectrum resource is scarce, H-CRAN scene can cover more users. In three schemes, the throughput performance comparisons among one-tier HPN, one-tier office RRH, one-tier house RRH, one-tier C-RAN, and two-tier H-CRAN are consistent. On the other hand, throughput performance of the proposed scheme is slightly below the optimal throughput scheme, which is the suboptimal. Traditional heterogeneous networks scheme has the lowest performance. Therefore, H-CRAN architecture is able to dispose the inter-layer CoMP between HPN and RRH, which has been shown to be increasingly beneficial in increasing system throughput. Due to the fact that HPN provides seamlessly cover of burst communications business or instant messaging services and RRHs support local service, the throughput of HPN-tier is not great as other scenes.

Moreover, office RRH has higher degree of activity in "Office Hour". Most of the family RRHs are self-adaptive go into sleep mode and a substantial number of the office RUEs access to BBU pool. Therefore, office RRH has higher throughput than residential RRHs.

### B. Energy Efficiency

In an Office Hour, energy efficiency performance comparisons among one-tier HPN, one-tier office RRH, one-tier house RRH, one-tier C-RAN and two-tier H-CRAN are shown in Fig. 4 in three different schemes.

In Family Hour, energy efficiency performance comparisons among one-tier HPN, one-tier office RRH, one-tier house RRH, one-tier C-RAN and two-tier H-CRAN are shown in Fig. 5 in three different schemes.

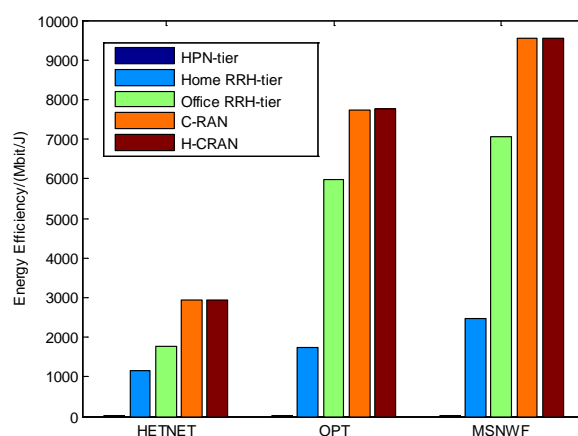


Fig.4 EE performance comparisons among one-tier HPN, one-tier office RRH, one-tier house RRH, one-tier C-RAN, and two-tier H-CRAN in "Office Hour".

Simulation results show that the EE performance of proposed scheme is greater than that of OPT algorithm. As shown in Fig. 4 and Fig. 5, EE performances are compared among the one-tier HPN, two-tier HETNET, one-tier office RRH, one-tier house RRH, one-tier C-RAN, and two-tier H-CRAN in different time period. Simulation results show that the EE in the two-tier H-CRAN scenario has the best performance. H-CRAN architecture is able to dispose the inter-layer CoMP between HPN and RRH, which has been shown to be increasingly beneficial in increasing system EE. EE performance of one-tier C-RAN is slightly worse than that of H-CRAN. On the other hand, EE of the proposed scheme perform far better than others, and OPT algorithm is the suboptimal one. Considering HPN with seamlessly cover of burst communications business or instant messaging services and RRHs with local service, the EE of HPN-tier is not great as other scenes. Moreover, the comparisons in Fig.4 and Fig.5 show that office RRH has higher degree of activity in "Office Hour". Most of the family RRHs are self-adaptive go into sleep mode and a substantial number of the office RUEs access to BBU pool. Therefore, the office RRH has higher EE than residential RRHs.

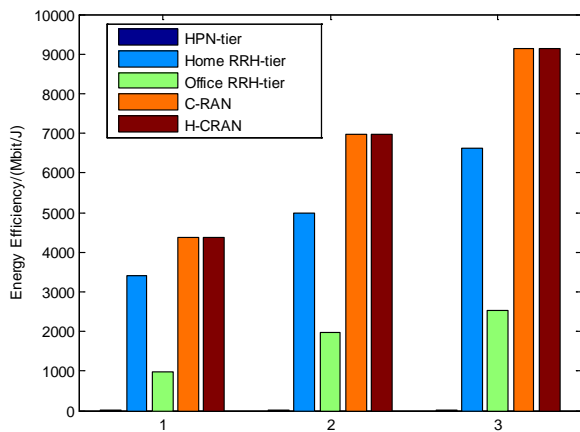


Fig.5 EE performance comparisons among one-tier HPN, one-tier office RRH, one-tier house RRH, one-tier C-RAN, and two-tier H-CRAN in "Family Hour".

### C. Activity Ratio of RRHs

The simulation results show that the activity ratio of office and residential users is different during office hours or family hours. Thus the throughput and energy efficiency are different. Because of the "tidal phenomenon" caused by human migration, the total number of people in the network is fixed, and the different periods are in different areas. As the office user activity increases, the activity of the home user reduces accordingly. When the activity ratio of house users increases, energy efficiency and throughput of office RRH and family RRH in HETNET, H-CRAN-Opt, H-CRAN-MSNWF change. The simulation results are shown in Fig.6 and Fig.7.

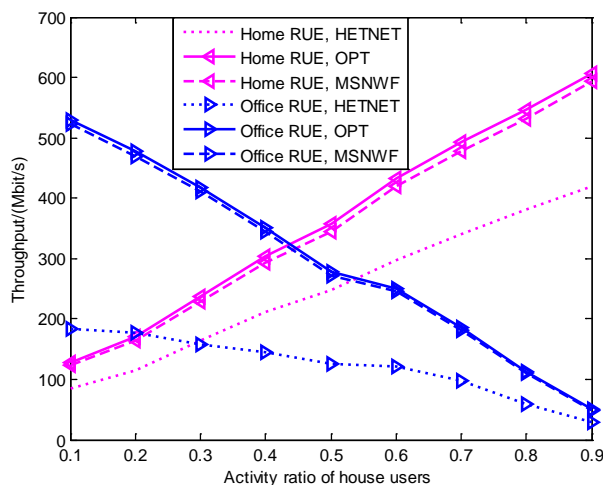


Fig.6 Throughput of office RRH-tier and residential RRH-tier vs. activity ratio of house users.

In terms of throughput, the scheme proposed in this paper is close to the optimal scheme of throughput. They all outperform the traditional scheme incredibly under activity ratio of house users.

With the higher activity ratio of residential users, the growth of throughput for residential users is more obvious. This means that residential users are more active, and have more active access to BBU pool. BBU processing pool generated higher

coordination gain. Thus throughput enhance more significantly. Therefore, with the increase of RRH users, the gap between the H-CRAN-MSNWF scheme and OPT algorithm slightly increases. According to the "tidal phenomenon", with the growth in the activity of office users, office RRH-tier throughput also increases and residential RRH-tier user throughput decreases. Under different activity ratio of office users, the overall throughput trend of HETNET, H-CRAN-Opt, H-CRAN-MSNWF are consistent.

With the higher activity ratio of house users, home users can access RRH adaptively. Under different activity ratio of users, the proposed scheme MSNWF has the best performance. With the higher activity ratio of residential users, the EE of residential users enhance the more obviously. This shows that residential users are more active, residential users more active access to BBU pool. BBU processing pool generates higher coordination gain. When the activity ratio of house users increases, a large number of office users migrate to the residence in Family Time. As the activity ratio of office users falls, energy efficiency of office RRH-tier declines and energy efficiency of residential RRH-tier rises. Under different activity ratio of office users, the overall energy efficiency trend of HETNET, H-CRAN-Opt, H-CRAN-MSNWF are consistent.

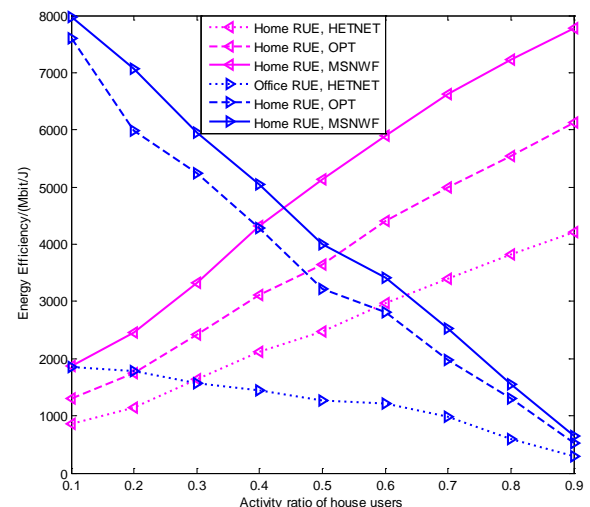


Fig.7 EE of office RRH-tier and residential RRH-tier vs. activity ratio of house users.

### D. Complexity analysis

Using the analysis in part C of section III, the complexity evaluated by the FLOPS of MSNWF and OPT are demonstrated in Fig.8. The total flop of MSNWF  $3n^2 + n \log_2 n + 15n$  is far less than the total flop of OPT  $9n^3 + 6n^2 + n$ . As shown in Fig.8, it is clear that the complexity is significantly improved by MSNWF in comparison to the OPT at about  $n > 2$ , especially when users number is large. Therefore, we can conclude that the MSNWF performs favorably than OPT in terms of computational complexity.



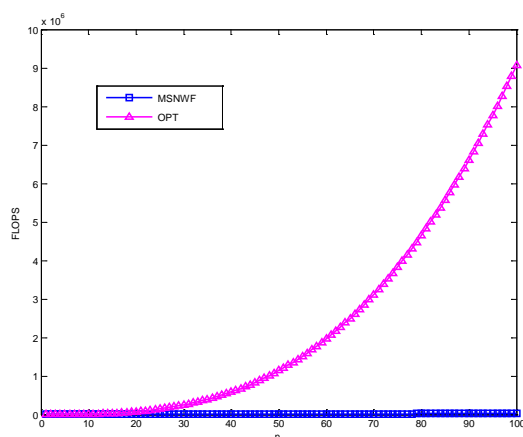


Fig.8 Performance of FLOPS for MSNWF and OPT

## V. CONCLUSION

Considering the architecture of H-CRAN, this paper focuses on the performance matrix of system throughput, EE and user activity. The EE performance is improved by reducing the complexity of matrix inversion calculation during beamforming and the power consumption of baseband. A low complexity scheme named as MSNWF has the best EE performance in one-tier office RRH, one-tier house RRH, one-tier C-RAN and two-tier H-CRAN. RRH can adaptively access BBU POOL in H-CRAN, which makes the system more robust to the "tidal phenomenon" caused by human migration. Moreover, compared with the traditional C-RAN, H-CRAN achieves better performance in throughput and energy efficiency under any activity ratio of users due to the realization of the inter-layer CoMP. The simulation analysis shows that the proposed scheme enhances the integral energy efficiency at the cost of a small part of the throughput. The proposed MSNWF applied for H-CRAN, which conforms to green communication, can decrease energy consumption.

## ACKNOWLEDGEMENT

This work was supported by the National Natural Science Foundation of China under Grant 61671183, Grant 61771163, and the Open Research Fund of CETC key laboratory of aerospace information applications under Grant SXX18629T022..

## REFERENCES

- [1] M. S. Mekala and P. Viswanathan, "A novel technology for smart agriculture based on IoT with cloud computing," *2017 International Conference on I-SMAC (IoT in Social, Mobile, Analytics and Cloud) (I-SMAC)*, Palladam, 2017, pp. 75-82.
- [2] J. A. Stankovic, "Research Directions for the Internet of Things," in *IEEE Internet of Things Journal*, vol. 1, no. 1, pp. 3-9, Feb. 2014.
- [3] J. Lin, W. Yu, N. Zhang, X. Yang, H. Zhang and W. Zhao, "A Survey on Internet of Things: Architecture, Enabling Technologies, Security and Privacy, and Applications," in *IEEE Internet of Things Journal*, vol. 4, no. 5, pp. 1125-1142, Oct. 2017.
- [4] J. Xu, K. Ota and M. Dong, "Real-Time Awareness Scheduling for Multimedia Big Data Oriented In-Memory Computing," in *IEEE Internet of Things Journal*.
- [5] E. Fitzgerald, M. Pióro and A. Tomaszewski, "Energy-Optimal Data

- Aggregation and Dissemination for the Internet of Things," in *IEEE Internet of Things Journal*, vol. PP, no. 99, pp. 1-1.
- [6] D. Zhai, R. Zhang, L. Cai, B. Li and Y. Jiang, "Energy-Efficient User Scheduling and Power Allocation for NOMA based Wireless Networks with Massive IoT Devices," in *IEEE Internet of Things Journal*, vol. PP, no. 99, pp. 1-1.
- [7] J. Wu, J. Thompson, H. Zhang, R. V. Prasad and S. Guo, "Green Communications and Computing Networks," in *IEEE Communications Magazine*, vol. 55, no. 11, pp. 12-13, NOVEMBER 2017.
- [8] H. Zhou, W. Xu, Y. Bi, J. Chen, Q. Yu and X. S. Shen, "Toward 5G Spectrum Sharing for Immersive-Experience-Driven Vehicular Communications," in *IEEE Wireless Communications*, vol. 24, no. 6, pp. 30-37, Dec. 2017.
- [9] Y. Wu, V. K. N. Lau, D. H. K. Tsang and L. Qian, "Energy-efficient transmission strategy for Cognitive Radio systems," *2012 IEEE Wireless Communications and Networking Conference Workshops (WCNCW)*, Paris, 2012, pp. 41-46.
- [10] Y. Wu, J. Wang, L. Qian and R. Schober, "Optimal Power Control for Energy Efficient D2D Communication and Its Distributed Implementation," in *IEEE Communications Letters*, vol. 19, no. 5, pp. 815-818, May 2015.
- [11] M. Jia, Z. Yin, Q. Guo, G. Liu and X. Gu, "Downlink Design for Spectrum Efficient IoT Network," in *IEEE Internet of Things Journal*, vol. PP, no. 99, pp. 1-1.
- [12] L. P. Qian, Y. Wu, H. Zhou and X. Shen, "Joint Uplink Base Station Association and Power Control for Small-Cell Networks With Non-Orthogonal Multiple Access," in *IEEE Transactions on Wireless Communications*, vol. 16, no. 9, pp. 5567-5582, Sept. 2017.
- [13] M. Peng, Y. Li, Z. Zhao and C. Wang, "System architecture and key technologies for 5G heterogeneous cloud radio access networks," in *IEEE Network*, vol. 29, no. 2, pp. 6-14, March-April 2015.
- [14] O. Simeone, A. Maeder, M. Peng, O. Sahin and W. Yu, "Cloud radio access network: Virtualizing wireless access for dense heterogeneous systems," in *Journal of Communications and Networks*, vol. 18, no. 2, pp. 135-149, April 2016.
- [15] W. Xu, H. Zhou, W. Shi, F. Lyu and X. Shen, "Throughput Analysis of In-Vehicle Internet Access via On-Road WiFi Access Points," *2017 IEEE 86th Vehicular Technology Conference (VTC-Fall)*, Toronto, ON, 2017, pp. 1-5.
- [16] M. Peng, H. Xiang, Y. Cheng, S. Yan and H. V. Poor, "Inter-Tier Interference Suppression in Heterogeneous Cloud Radio Access Networks," in *IEEE Access*, vol. 3, pp. 2441-2455, 2015.
- [17] J. Tang, R. Wen, T. Q. S. Quek and M. Peng, "Fully Exploiting Cloud Computing to Achieve a Green and Flexible C-RAN," in *IEEE Communications Magazine*, vol. 55, no. 11, pp. 40-46, NOVEMBER 2017.
- [18] M. Sheng, Y. Wang, J. Li, R. Liu, D. Zhou and L. He, "Toward a Flexible and Reconfigurable Broadband Satellite Network: Resource Management Architecture and Strategies," in *IEEE Wireless Communications*, vol. 24, no. 4, pp. 127-133, Aug. 2017.
- [19] M. Peng, K. Zhang, J. Jiang, J. Wang and W. Wang, "Energy-Efficient Resource Assignment and Power Allocation in Heterogeneous Cloud Radio Access Networks," in *IEEE Transactions on Vehicular Technology*, vol. 64, no. 11, pp. 5275-5287, Nov. 2015.
- [20] S. Luo, R. Zhang and T. J. Lim, "Downlink and Uplink Energy Minimization Through User Association and Beamforming in C-RAN," in *IEEE Transactions on Wireless Communications*, vol. 14, no. 1, pp. 494-508, Jan. 2015.
- [21] D. Sabella et al., "Energy Efficiency Benefits of RAN-as-a-Service Concept for a Cloud-Based 5G Mobile Network Infrastructure," in *IEEE Access*, vol. 2, pp. 1586-1597, 2014.
- [22] G. Nain, S. S. Das and A. Chatterjee, "Low Complexity User Selection With Optimal Power Allocation in Downlink NOMA," in *IEEE Wireless Communications Letters*, vol. 7, no. 2, pp. 158-161, April 2018..
- [23] M. Ali, Q. Rabbani, M. Naem, S. Qaisar and F. Qamar, "Joint User Association, Power Allocation, and Throughput Maximization in 5G H-CRAN Networks," in *IEEE Transactions on Vehicular Technology*, vol. 66, no. 10, pp. 9254-9262, Oct. 2017.
- [24] I. Alqerm and B. Shihada, "Sophisticated Online Learning Scheme for Green Resource Allocation in 5G Heterogeneous Cloud Radio Access Networks," in *IEEE Transactions on Mobile Computing*, vol. 17, no. 10, pp. 2423-2437, 1 Oct. 2018.
- [25] S. Li, G. Zhu, S. Lin, Q. Gao, S. Xu and L. Xiong, "Energy-Efficient Power Allocation in Cloud Radio Access Network of High-Speed Railway," *2016 IEEE 83rd Vehicular Technology Conference (VTC)*

- Spring), Nanjing, 2016, pp. 1-5.
- [26] F. Boccardi and H. Huang, "Zero-Forcing Precoding for the MIMO Broadcast Channel under Per-Antenna Power Constraints," *2006 IEEE 7th Workshop on Signal Processing Advances in Wireless Communications*, Cannes, 2006, pp. 1-5.
  - [27] S. Fu et al., "Interference Cooperation via Distributed Game in 5G Networks," in *IEEE Internet of Things Journal*, vol. PP, no. 99, pp. 1-1.
  - [28] L. Chen, H. Jin, H. Li, J. B. Seo, Q. Guo and V. Leung, "An Energy Efficient Implementation of C-RAN in HetNet," *2014 IEEE 80th Vehicular Technology Conference (VTC2014-Fall)*, Vancouver, BC, 2014, pp. 1-5.
  - [29] B. Ismaiel, M. Abolhasan, W. Ni, D. Smith, D. Franklin and A. Jamalipour, "Analysis of Effective Capacity and Throughput of Polling Based Device-To-Device Networks," in *IEEE Transactions on Vehicular Technology*.
  - [30] S. Bassoy, M. Jaber, M. A. Imran and P. Xiao, "Load Aware Self-Organising User-Centric Dynamic CoMP Clustering for 5G Networks," in *IEEE Access*, vol. 4, pp. 2895-2906, 2016.
  - [31] M. Peng, Y. Yu, H. Xiang and H. V. Poor, "Energy-Efficient Resource Allocation Optimization for Multimedia Heterogeneous Cloud Radio Access Networks," in *IEEE Transactions on Multimedia*, vol. 18, no. 5, pp. 879-892, May 2016.
  - [32] Q. Liu, G. Wu, Y. Guo, Y. Zhang and S. Hu, "Energy Efficient Resource Allocation for Control Data Separated Heterogeneous-CRAN," *2016 IEEE Global Communications Conference (GLOBECOM)*, Washington, DC, 2016, pp. 1-6.
  - [33] C. Desset et al., "Flexible power modeling of LTE base stations," *2012 IEEE Wireless Communications and Networking Conference (WCNC)*, pp. 2858-2862, Apr. 2012.
  - [34] G. Auer et al., "D2.3: Energy efficiency analysis of the reference systems, areas of improvements and target breakdown," INFOS-ICT-247733 Earth (Energy Aware Radio and NeTwork Technologies), Tech. Rep., Nov. 2010.
  - [35] AvagoTechnologies. Digital Diagnostic SFP, 850nm 3.072/2.4576 Gb/s, RoHS OBSAI/CPRI Compatible Optical Transceiver. Avago Technologies AFBR-57J5APZ. 2013
  - [36] Hu R Q, Qian Y. 13. Evolution of HetNet Technologies in LTE-Advanced Standards Heterogeneous Cellular Networks. John Wiley Sons Ltd, 2013:287-311.
  - [37] V. F. Crășmariu, M. O. Arvinte, A. A. Enescu and S. Ciochină, "Waterfilling power allocation applied in block-diagonalization Multi-User MIMO precoding technique," *2016 12th IEEE International Symposium on Electronics and Telecommunications (ISETC)*, Timisoara, 2016, pp. 91-94.



**Xuemai Gu** received his M.Sc. and Ph.D. from the Department of Information and Communication Engineering, HIT in 1985 and 1991, respectively. He is currently a professor and president of the Graduate School of HIT. His research interests focus on integrated and hybrid satellite and terrestrial communications and broadband multimedia communication technique.



**Qing Guo** received his M.Sc. and Ph.D. from Beijing University of Posts and Telecommunications and HIT in 1985 and 1998, respectively. He is currently a professor and president at the School of Electronics and Information Engineering, HIT. His research interests focus on satellite communications and broadband multimedia communication techniques.



**Ximu Zhang** received her M.Sc degree in Harbin Institute of Technology (HIT), in 2017. She is currently a Ph.D candidate student in Communication Research Center and School of Electronics and Information Engineering, HIT. Her research interests include broadband satellite communications and heterogeneous cloud radio access network.



**Min Jia** received her M.Sc degree in information and communication engineering from Harbin Institute of Technology (HIT) in 2006, and her Ph.D. degree from SungKyungKwan University of Korea and HIT in 2010. She is currently an associate professor and Ph.D supervisor at the Communication Research Center and School of Electronics and Information Engineering, HIT. Her research interests focus on advanced mobile communication technology and non-orthogonal transmission scheme for 5G, cognitive radio, digital signal processing, machine learning and

broad-band satellite communications.